08

Influence of heterostructure radius increment on the heterointerface of $IIIV_xV_{1-x}$ nanowires

© E.D. Leshchenko[1], V.G. Dubrovskii[2]

[1] Submicron Heterostructures for Microelectronics, Research & Engineering Center, RAS, Saint-Petersburg, Russia
[2] St. Petersburg State University, St. Petersburg, Russia
E-mail: leshchenko.spb@gmail.com

Received September 3, 2025
Revised October 3, 2025
Accepted October 3, 2025

The formation of axial heterostructures in $IIIV_xV_{1-x}$ nanowires is studied theoretically. We consider the case when the nanowire radius changes during the growth. It is shown that an increase in the radius has almost no effect on the heterointerface of thin nanowires. The effect becomes noticeable at a high rate of radial growth or for thick nanostructures. It is shown that the radius increment during growth leads to the formation of a sharper heterojunction, which is especially pronounced in nanostructures with a large radius.

Keywords: modelling, nanowires, III−V−V heterostructures, interfacial profile.

DOI: 10.61011/TPL.2026.02.63036.20488

Since their first synthesis in 1995 [1], axial heterostructures based on nanowires (NWs) have attracted considerable interest due to their unique electronic, optical, and mechanical properties. The wide functionality of heterostructures has led to their use in various types of devices, including field-effect transistors [2], photodetectors [3], light-emitting diodes [4], lasers [5], and solar batteries [6]. The heterojunction abruptness is one of the key characteristics of heterostructures that affects the efficiency of devices. Owing to the reservoir effect, growth materials accumulate in a catalyst droplet [7], which leads to blurring of heteroboundaries (especially in III−III−V systems [8]). This effect may be overcome with the use of short pulsed fluxes of atoms or molecules [7] or by stopping growth at the moment of gas flux switching [9]. A complete change in droplet composition during growth arrest provides an opportunity to synthesize InAs/GaAs heterostructures based on NWs with atomically sharp heterojunctions [10]. *In situ* transmission electron microscopy studies provide extensive data on the dynamics of heterostructure formation [11].

Modeling of the process of formation of heterostructures based on NWs is aimed primarily at establishing the relation between the compositional profile of the heterojunction and growth parameters. Most models are a combination of the material balance in a droplet and the mode of incorporation of atoms into NWs and are divided into four groups [12]: equilibrium [13], nucleation-limited [14], kinetic [15], and regular growth [16] ones. In one of the more recent studies [17], the process of formation of heterostructures was analyzed based on a self-consistent model that takes into account such elementary processes as gas flux into a droplet, desorption of group V atoms in the form of dimers, and NW growth. However, it was assumed in [17] (as in most other works [12–16]) that the NW radius does not change during growth. This assumption is often violated, especially during the synthesis of heterostructures based on NWs containing antimony (e.g., $GaAs/GaAs_{1-x}Sb_x$ [18,19], $InAs/InAs_{1-x}Sb_x$ [20], and $InSb/Ga_xIn_{1-x}Sb$ [21]). A more than 1.5-fold increase in radius was also observed in growth of InAs/InP heterostructures based on NWs [22]. The present study is aimed at examining the influence of increasing NW radius on the formation of heterostructures in III−V−V NWs.

Most axial heterostructures based on NWs are grown by the vapor–liquid–solid mechanism [23]. Common epitaxy methods include metalorganic vapor-phase epitaxy [24] and molecular beam epitaxy [25]. The growth of an axial heterostructure starts with the formation of a catalyst droplet. One widely used catalyst material is Au [23] (gold is denoted as element U in Fig. 1). However, the

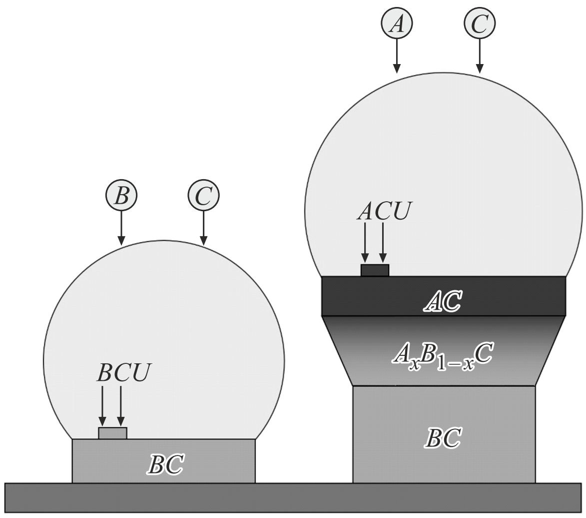

Figure 1. Diagram of growth of NW-based heterostructure BC/AC.

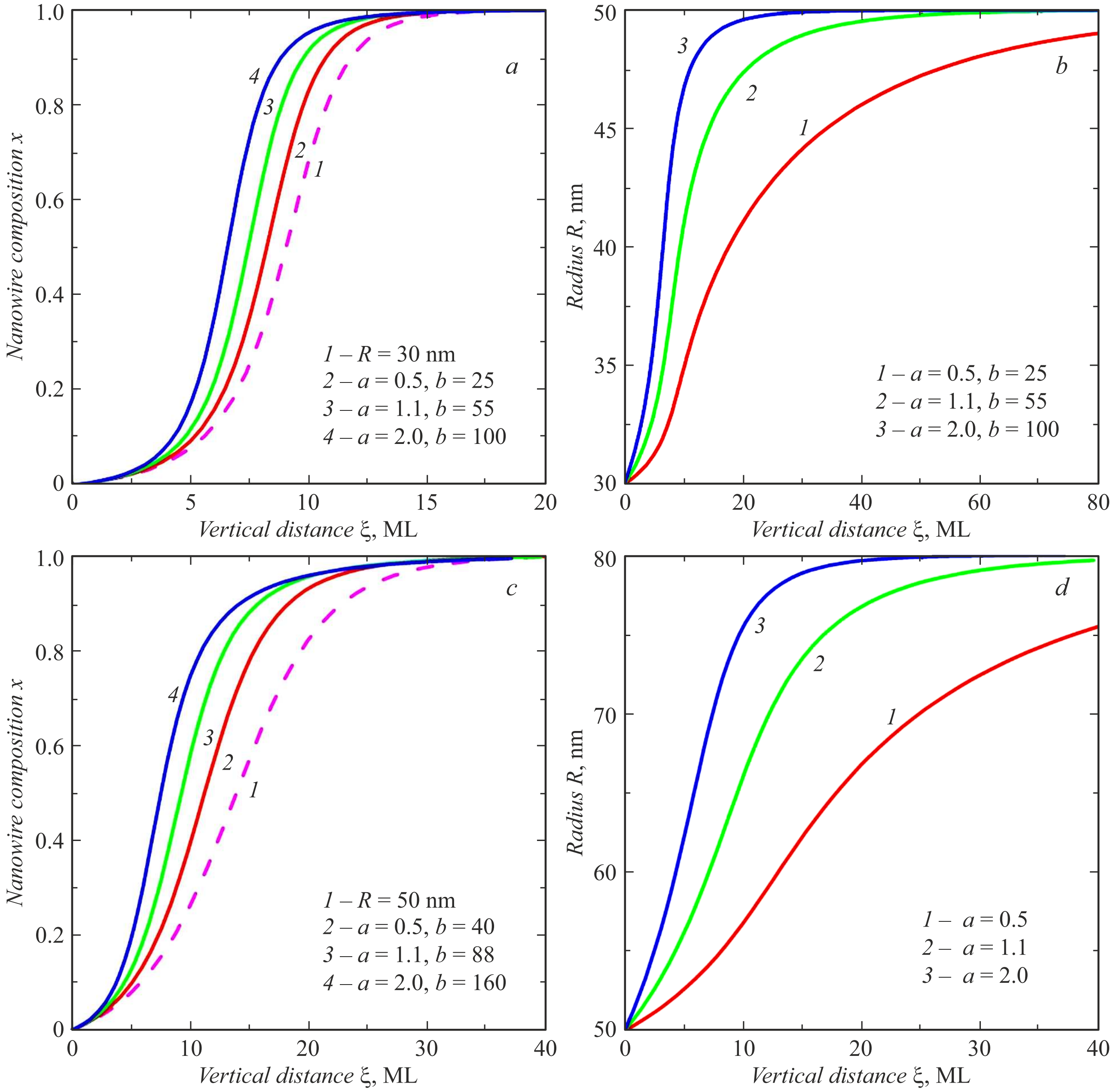

Figure 2. *a*, *c* — Composition profiles of the $BC/A_xB_{1-x}C$ heterojunction in NWs calculated at different radial growth rates and initial radii $R_0 = 30$ and 50 nm, respectively. Dashed curves correspond to heterostructures with constant radius $R = 30$ (*a*) and 50 nm (*c*). *b*, *d* — Dependences of the nanostructure radius on the coordinate along the NW axis calculated for initial radii $R_0 = 30$ and 50 nm, respectively.

droplet may consist of a group III element that is part of the NW (i.e., growth may proceed without an external catalyst). This type of synthesis is called self-catalyzed [26]. When the semiconductor material is deposited, atoms B and C enter the droplet, inducing (under the condition of its supersaturation) the formation of NW BC. One of the ways to form heterojunction $BC/A_xB_{1-x}C$ is to substitute the flux of B atoms with a flux of A atoms. The number of B atoms in the droplet decreases with time, while the AC concentration in the NW increases. At zero concentration of B atoms, NW AC is synthesized. The discussed growth diagram is presented in Fig. 1.

From material balance considerations [17], equations characterizing the change in number of atoms of group V elements N_i $(i = A, B)$ in the droplet are written as

$$\frac{dN_i}{dt} = V_i - V_i^{des} - K_i\chi_i. \quad (1)$$

Here, V_i is the gas flux of atoms, V_i^{des} is the desorption flux, K_i is the crystallization rate of pairs AC and BC, t is time,

$\chi_i = N_i/N_{tot}$ is the concentration of element i in the droplet, and $N_{tot} = N_A + N_B + N_C + N_U$, where N_C and N_U are the numbers of atoms C and U in the droplet, respectively. The vertical growth rate may be determined from equation

$$\frac{\pi R^2 h}{\Omega_s}\frac{d\xi}{dt} = K_A\chi_A + K_B\chi_B, \qquad (2)$$

where h is the monolayer height, Ω_s is the volume of the III–V pair in the solid phase, R — is the NW radius, and ξ is the coordinate along the NW axis in monolayers (ML). The gas flux of atoms and the desorption flux are specified by equations

$$V_i = \frac{h}{\Omega_s}\sigma_i v_i \frac{2\pi R^2}{1+\cos\beta}, \qquad (3)$$

$$V_i^{des} = \frac{h}{\Omega_s}\sigma_i v_i^{des}\frac{2\pi R^2}{1+\cos\beta}\chi_i^2, \qquad (4)$$

where σ_i are the condensation coefficients, β is the contact angle, v_i is the deposition rate of group V atoms, and v_i^{des} is the desorption rate [27]. The variation of number of atoms of group V elements in the droplet may be presented as

$$\frac{dN_i}{dt} = N_{tot}\frac{d\chi_i}{dt} + \chi_i\frac{dN_{tot}}{dt}. \qquad (5)$$

Relying on the assumptions of small concentrations of group V atoms ($N_{tot} \approx N_C + N_U$) and $N_{tot} \approx \pi R^3 f(\beta)/(3\Omega_l)$, where $f(\beta)$ is a function depending on the contact angle [27] and Ω_l is the volume of a group III atom in liquid, one may write the equations characterizing the rate of vertical growth and the change in concentration of group V atoms in the following form:

$$\frac{d\xi}{dt} = g_A\chi_A + g_B\chi_B, \qquad (6)$$

$$\frac{d\chi_i}{dt} = \gamma\left(\Phi_i - \Phi_i^{des}\chi_i^2 - g_i\chi_i - \frac{3}{R\gamma}\frac{dR}{dt}\chi_i\right). \qquad (7)$$

The coefficients here are

$$\Phi_i = \frac{2\sigma_i}{1+\cos\beta}v_i, \qquad (8)$$

$$\Phi_i^{des} = \frac{2\sigma_i}{1+\cos\beta}v_i^{des}, \qquad (9)$$

$$\gamma = \frac{3\Omega_l h}{\Omega_s R f(\beta)}, \qquad (10)$$

$$g_i = \frac{\Omega_s}{\pi R^2 h}K_i. \qquad (11)$$

Composition x of the ternary NW is specified by one-parameter ($c_l = g_A/g_B$) equation [27]:

$$x = \frac{\chi_A}{\chi_A + \chi_B/c_l}. \qquad (12)$$

Let us first compare the composition profiles of the heterojunction at constant and varying radii (Figs. 2, *a* and *c*). Theoretical curves were obtained by solving Eqs. (6) and (7) numerically with parameters $\gamma R = 0.0675$ nm, $\Phi_A = 1$ ML/s, $\Phi_B = 0$ ML/s, $\Phi_A^{des} = \Phi_B^{des} = 100$ ML/s, $g_A R^2 = 9000$ nm^2/s, $c_l = 0.1$, and initial concentrations $\chi_A^0 = 0$ and $\chi_B^0 = 0.02$. Approximate dependence $dR/dt = -a + b/R$ [28] at initial radii $R_0 = 30$ nm (Fig. 2, *a*) and 50 nm (Fig. 2, *c*) was used as the radial growth rate. It is evident from Fig. 2, *a* that a slow increase in NW radius ($dR/dt = -0.5 + 25/R$) does not induce any significant changes in the heterojunction profile of thin NWs ($R_0 = 30$ nm). However, the curves deviate significantly when the radial growth rate is high ($dR/dt = -2 + 100/R$). The discrepancy becomes even more pronounced if the initial radius is larger (Fig. 2, *c*). It follows from a comparison of Figs. 2, *a* and *c* that the thinner the NW is, the more abrupt is the heterojunction. The dependences of the NW radius on the coordinate along the nanostructure axis calculated at different radial growth rates are shown in Fig. 2, *b* ($R_0 = 30$ nm) and Fig. 2, *d* ($R_0 = 50$ nm). Parameters a and b were chosen so that the stationary radius to which the NW tends was 50 nm (Fig. 2, *b*) and 80 nm (Fig. 2, *d*).

Figure 3 illustrates the influence of the ratio of incorporation rates (c_l) on the heterojunction abruptness. It can be seen the heterojunction becomes more abrupt when the rate of incorporation of B atoms increases. In all the presented cases, an increase in heterostructure radius during growth leads to the formation of NWs with a more abrupt heterojunction.

The formation of III–V–V heterostructures was studied theoretically based on a model that takes into account the change in nanostructure radius during growth. It was found that the heterojunction abruptness of thin NWs

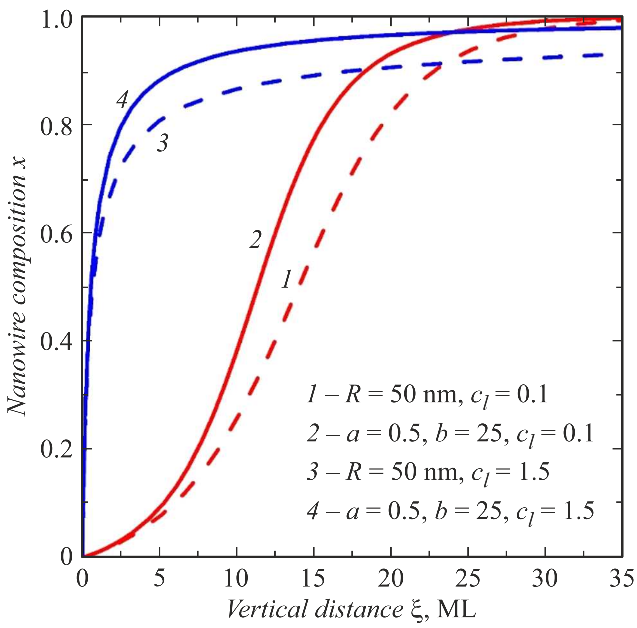

Figure 3. Composition profiles of the $BC/A_xB_{1-x}C$ heterojunction in NWs calculated for crystallization rate ratios $c_l = 0.1$ and 1.5. Dashed curves correspond to heterostructures with constant radius $R = 50$ nm.

changes insignificantly when the NW radius increases. The contribution associated with radial growth needs to be taken into account if the NW radius changes rapidly or if the NW radius is large. It was demonstrated that the heterojunction becomes more abrupt as the ratio of BC and AC crystallization rates increases. The obtained results may be used to optimize the growth parameters of heterostructures based on NWs with a predetermined heterojunction profile.

Funding

V.G. Dubrovskii wishes to thank the St. Petersburg State University (research grant ID 129360164) for financial support of analytical research.

Conflict of interest

The authors declare that they have no conflict of interest.

References

[1] K. Hiruma, H. Murakoshi, M. Yazawa, T. Katsuyama, J. Cryst. Growth, **163**, 226 (1996). DOI: 10.1016/0022-0248(95)00714-8
[2] H.A. Nilsson, P. Caroff, E. Lind, M.-E. Pistol, C. Thelander, L.-E. Wernersson, J. Appl. Phys., **110**, 064510 (2011). DOI: 10.1063/1.3633742
[3] M. Spies, E. Monroy, Semicond. Sci. Technol., **34**, 053002 (2019). DOI: 10.1088/1361-6641/ab0cb8
[4] R. Ha, S.-W. Kim, H.-J. Choi, Nanoscale Res. Lett., **8**, 299 (2013). DOI: 10.1186/1556-276X-8-299
[5] D. Ren, L. Ahtapodov, J.S. Nilsen, J. Yang, A. Gustafsson, J. Huh, G.J. Conibeer, A.T.J. van Helvoort, B.O. Fimland, H. Weman, Nano Lett., **18**, 2304 (2018). DOI: 10.1021/acs.nanolett.7b05015
[6] D. Alcer, M. Tirrito, L. Hrachowina, M.T. Borgstrom, ACS Appl. Nano Mater., **7**, 2352 (2024). DOI: 10.1021/acsanm.3c05909
[7] K.A. Dick, J. Bolinsson, B.M. Borg, J. Johansson, Nano Lett., **12**, 3200 (2012). DOI: 10.1021/nl301185x
[8] V. Zannier, D. Ercolani, U.P. Gomes, J. David, M. Gemmi, V.G. Dubrovskii, L. Sorba, Nano Lett., **16**, 7183 (2016). DOI: 10.1021/acs.nanolett.6b03524
[9] G. Priante, G. Patriarche, F. Oehler, F. Glas, J.-C. Harmand, Nano Lett., **15**, 6036 (2015). DOI: 10.1021/acs.nanolett.5b02224
[10] D. Scarpellini, C. Somaschini, A. Fedorov, S. Bietti, C. Frigeri, V. Grillo, L. Esposito, M. Salvalaglio, A. Marzegalli, F. Montalenti, E. Bonera, P.G. Medaglia, S. Sanguinetti, Nano Lett., **15**, 3677 (2015). DOI: 10.1021/nl504690r
[11] M. Marnauza, R. Sjökvist, A. Kraina, D. Jacobsson, K.A. Dick, ACS Nanosci. Au, **5**, 208 (2025). DOI: 10.1021/acsnanoscienceau.5c00015
[12] E.D. Leshchenko, N.V. Sibirev, Nanomaterials, **14**, 1816 (2024). DOI: 10.3390/nano14221816.
[13] G. Priante, F. Glas, G. Patriarche, K. Pantzas, F. Oehler, J.-C. Harmand, Nano Lett., **16**, 1917 (2016). DOI: 10.1021/acs.nanolett.5b05121
[14] V.G. Dubrovskii, A.A. Koryakin, N.V. Sibirev, Mater. Des., **132**, 400 (2017). DOI: 10.1016/j.matdes.2017.07.012
[15] E.D. Leshchenko, V.G. Dubrovskii, Nanotechnology, **34**, 065602 (2023). DOI: 10.1088/1361-6528/aca1c9
[16] V.G. Dubrovskii, N.V. Sibirev, Cryst. Growth Des., **16**, 2019 (2016). DOI: 10.1021/acs.cgd.5b01613
[17] V.G. Dubrovskii, Nanomaterials, **14**, 821 (2024). DOI: 10.3390/nano14100821
[18] S.G. Ghalamestani, M. Ek, M. Ghasemi, P. Caroff, J. Johansson, K.A. Dick, Nanoscale, **6**, 1086 (2014). DOI: 10.1039/c3nr05079c
[19] L. Li, L. Pan, Y. Xue, X. Wang, M. Lin, D. Su, Q. Zhang, X. Yu, H. So, D. Wei, B. Sun, P. Tan, A. Pan, J. Zhao, Nano Lett., **17**, 622 (2017). DOI: 10.1021/acs.nanolett.6b03326
[20] M. Borg, K.A. Dick, J. Eymery, L.-E. Wernersson, Appl. Phys. Lett., **98**, 113104 (2011). DOI: 10.1063/1.3566980
[21] S.G. Ghalamestani, M. Ek, M. Ghasemi, B. Ganjipour, C. Thelander, J. Johansson, P. Caroff, K.A. Dick, Nano Lett., **12**, 4914 (2012). DOI: 10.1021/nl302497r
[22] V. Zannier, F. Rossi, V.G. Dubrovskii, D. Ercolani, S. Battiato, L. Sorba, Nano Lett., **18**, 167 (2018). DOI: 10.1021/acs.nanolett.7b03742
[23] R.S. Wagner, W.C. Ellis, Appl. Phys. Lett., **4**, 89 (1964). DOI: 10.1063/1.1753975
[24] P. Caroff, M.E. Messing, M. Borg, K.A. Dick, K. Deppert, L.E. Wernersson, Nanotechnology, **20**, 495606 (2009). DOI: 10.1088/0957-4484/20/49/495606
[25] F. Jabeen, S. Rubini, F. Martelli, Microelectronics J., **40**, 442 (2009). DOI: 10.1016/j.mejo.2008.06.001
[26] P. Krogstrup, R. Popovitz-Biro, E. Johnson, M.H. Madsen, J. Nygård, H. Shtrikman, Nano Lett., **10**, 4475 (2010). DOI: 10.1021/nl102308k
[27] F. Glas, M.R. Ramdani, G. Patriarche, J.-C. Harmand, Phys. Rev. B, **88**, 195304 (2013). DOI: 10.1103/PhysRevB.88.195304
[28] V.G. Dubrovskii, T. Xu, A. Diaz Alvarez, S.R. Plissard, P. Caroff, F. Glas, B. Grandidier, Nano Lett., **15**, 5580 (2015). DOI: 10.1021/acs.nanolett.5b02226

Translated by D.Safin